

Electromagnetic vibrations estimation of an induction motor by nonlinear optimal filtering

Pierre Granjon

Laboratory of Images and Signals (LIS), INP Grenoble,
38402 St Martin d'Hères, France

Phone: +33-476827132 Fax: +33-476826384

Email: pierre.granjon@lis.inpg.fr

Abstract—Stator frame radial vibrations of an induction motor are composed of the sum of three different components: aerodynamic, mechanical and electromagnetic vibrations. The separation of these components could be useful in order to quantify their respective vibratory influence. Moreover, each of these components carrying different physical informations, such a processing could be interesting to further analyze each component independently, and finally diagnose induction machine faults more easily. This paper deals with a new processing algorithm able to extract electromagnetic vibrations of an induction motor from measured signals. To this end, a nonlinear quadratic optimal filter is used to estimate these vibratory components from stator currents and radial vibrations measured at one location on the stator frame. This algorithm is based on the physical quadratic link between stator currents and electromagnetic vibrations, which is first detailed. The algorithm used to estimate the optimal nonlinear quadratic filter is then determined and analyzed. Finally, the proposed algorithm is applied to real signals, and is shown to be very efficient, whatever frequency band.

Index Terms—induction motor, radial vibrations, electromagnetic vibrations, nonlinear optimal filtering, diagnostic.

I. PROBLEM STATEMENT AND PHYSICAL MODELING

Radial vibrations $v(t, \theta)$ of an electrical motor measured at time t and angular position θ on the stator frame are usually modeled as the sum of three terms, each of which having a different physical origin [1], [2]:

$$v(t, \theta) = v_a(t, \theta) + v_m(t, \theta) + v_e(t, \theta), \quad (1)$$

where:

- $v_a(t, \theta)$ are aerodynamic vibrations, generated by pressure variations in the air gap,
- $v_m(t, \theta)$ are mechanical vibrations, due to the rotation of different parts of the machine (rotor, bearings, ...),
- $v_e(t, \theta)$ are electromagnetic vibrations, caused by the electromagnetic force related to the magnetic field in the air gap.

In order to simplify radial vibrations $v(t, \theta)$, and to quantify the vibratory influence of the different physical phenomena, a useful processing would be to separate the three previous components ($v_a(t, \theta)$, $v_m(t, \theta)$ and $v_e(t, \theta)$) from each other. The present work can be considered as the first step of this processing, since its aim is to extract electromagnetic vibrations $v_e(t, \theta)$ from radial vibrations.

To this end, the modelization of electromagnetic vibrations has to be further detailed. Firstly, stator currents $i_s(t)$ supply-

ing the machine induces a magnetic field $b(t, \theta)$ in the air-gap. Since this phenomenon is supposed to be linear in the present work, these two quantities mostly have the same spectral content. Secondly, this field generates a radial force density $\sigma(t, \theta)$ between rotor and stator frame, which is quadratically related to $b(t, \theta)$ thanks to the Maxwell stress method [3], [4]:

$$\sigma(t, \theta) = \frac{b^2(t, \theta)}{2\mu_0}, \quad \text{with } \mu_0 = 4\pi 10^{-7}. \quad (2)$$

This equation shows that this force density $\sigma(t, \theta)$ has the same spectral content that squared stator currents. Finally, the stator frame is commonly modeled as a linear time-invariant (LTI) mechanical system. Its input is the previous force density and its output the electromagnetic vibrations [1], [2]. From the above considerations, we can state that electromagnetic vibrations $v_e(t, \theta)$ are related to stator currents $i_s(t)$ through a nonlinear quadratic system. Fig. 1 schematically represents the structure of the quadratic nonlinear system chosen to modelize radial vibrations of an electrical machine.

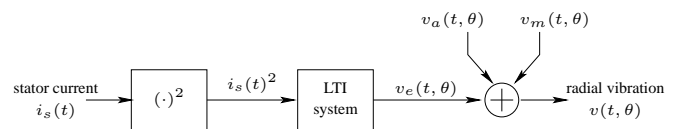


Fig. 1. Physical modeling of radial vibrations of an induction machine

Stator currents $i_s(t)$ and radial vibrations $v(t, \theta)$ are two easily measured quantities on real machines. The aim of this work is to elaborate an optimal filter to estimate $v_e(t, \theta)$ from these two measured quantities. The theoretical form of this optimal filter (which has to be nonlinear as shown previously), and its estimation algorithm are determined in the next section.

II. OPTIMAL NONLINEAR FILTERING

For the sake of simplicity, the dependence of the different signals on the angular position θ will be omitted in the following.

The two only measured signals are one stator current $i_s(t)$, and stator frame radial vibrations $v(t)$. They are sampled at sampling frequency f_s , and their sampled versions $i_s(n)$ and

$v(n)$ are supposed to verify Shannon's sampling theorem. The physical model given in section I and represented in Fig. 1 can be used to determine the global structure of the algorithm necessary to estimate electromagnetic vibrations $v_e(n)$ from $i_s(n)$ and $v(n)$:

Step 1: determine $i_s^2(n)$ from $i_s(n)$,

Step 2: determine an optimal linear filter to estimate the LTI system of Fig. 1 from $i_s^2(n)$ and $v(n)$.

These two steps, detailed in the following subsections, allow to estimate an optimal nonlinear quadratic filter in order to modelize the nonlinear system described in the previous section.

A. Step 1: determine $i_s^2(n)$ from $i_s(n)$

This first step is a nonlinear operation, which induces frequency shifts in numerical signals. For example, if the signal $i_s(n)$ contains different frequency components between 0 and $f_s/2$, the spectrum of its squared version $i_s^2(n)$ spreads from 0 to f_s . This squared signal is subject to spectral overlapping since it does not verify Shannon's sampling theorem any more. To prevent this phenomenon, the numerical signal $i_s(n)$ can be upsampled by a factor 2 before the squaring operation. Indeed, this upsampling confines the spectrum of the upsampled signal between 0 and $f_s/4$ [5], which can be squared without any spectral overlapping. In order to obtain a signal with a sampling frequency f_s at the output of this nonlinear operation, the squared signal has to be downsampled by the same factor 2. This principle is illustrated in Fig. 3. The sampled signal given by this first

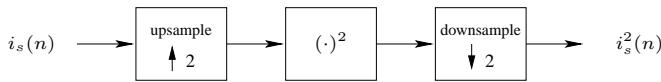


Fig. 3. Numerical implementation of a squaring operation

step is a correct numerical version of the squared signal $i_s^2(t)$ in the frequency band $[0, f_s/2]$.

B. Step 2: determine an optimal linear filter from $i_s^2(n)$ and $v(n)$

This second problem is equivalent to estimate the transfer function of the LTI system represented in Fig. 1 by using the known signals $i_s^2(n)$ and $v(n)$. Indeed, once this transfer function is known, electromagnetic vibrations are reconstructed by applying this filter to the squared stator current. This problem is solved by optimal filtering, also called Wiener filtering. This theory were originally applied in [6] in the time domain, but since stator currents are mostly periodic, this method is implemented here in the frequency domain. This algorithm has been extensively studied in the signal processing community, and a simple introduction can be found in [7], [8] while a more theoretic approach is given in [9].

Two hypothesis are necessary to use this method:

1. the system to identify has to be linear and time invariant,
2. its input has to be uncorrelated to the additive noise present on the measured signal.

The first hypothesis was already assumed during the development of the physical model described in section I. Concerning the second hypothesis, the input of the system is $i_s^2(n)$, generated by the power supply (power network and inverter) of the

machine. The measured signal is radial vibrations, where additive noise is $v_a(n) + v_m(n)$, generated by aerodynamic and mechanical phenomena in the machine. Thanks to their completely different physical origin, $i_s^2(n)$ and $v_a(n) + v_m(n)$ are obviously uncorrelated, and the two previous hypothesis are finally satisfied.

Under these assumptions, the transfer function of the filter which best estimates electromagnetic vibrations $v_e(n)$ from $i_s^2(n)$ is given by:

$$H_o(f) = \frac{\gamma_{vi_s^2}(f)}{\gamma_{i_s^2 i_s^2}(f)}, \quad (3)$$

where $\gamma_{i_s^2 i_s^2}(f)$ is the power spectral density (or power spectrum) of $i_s^2(n)$, and $\gamma_{vi_s^2}(f)$ is the cross spectral density (or cross power spectrum) between $v(n)$ and $i_s^2(n)$. This filter is called the optimal filter or Wiener filter. Its output, noted $\widehat{v_e(n)}$, is the best estimate of $v_e(n)$ in the least squares sense since it minimizes the mean squared error between these two signals. This filter is able to extract from measured vibrations $v(n)$ all the components correlated with $i_s^2(n)$, i.e. electromagnetic vibrations.

The transfer function of Eq. (3) can be calculated from the known signals $i_s^2(n)$ and $v(n)$ by estimating their power and cross spectral densities. In the following, these spectral quantities will be estimated through the Welch modified periodogram.

Fig. 2 schematically represents the complete algorithm previously established, which is applied on real signals in the next section.

III. EXPERIMENTAL RESULTS

This experiment was carried out on a 5 kW, four-pole, three-phase induction motor with 24 rotor slots. It was supplied by a pulsewidth modulation (PWM) inverter, with a switching frequency $f_{PWM} = 5$ kHz. The machine was in steady state, with a fundamental supply frequency $f_1 = 32$ Hz, and a constant rotating frequency $f_r = 13.7$ Hz. One stator current and radial vibrations of the machine were measured by a current sensor and an accelerometer placed in the middle of the stator frame. These two signals were low-pass filtered between 0 and 12 kHz by an antialiasing filter and sampled at $f_s = 25.6$ kHz in order to verify Shannon's sampling theorem. The results obtained on these real signals are shown in the following figures.

Fig. 4 represents the power spectral density (PSD) of the measured stator current between 0 and 7000 Hz in dB, such that even small components are visible. This curve shows that this signal contains the following important harmonic components :

- supply frequency harmonics, situated in the low frequency band (0 – 300 Hz) and mainly constituted by the fundamental supply frequency ($f_1 = 32$ Hz) and its 5th and 7th harmonics,
- slot harmonics situated around multiples of $\simeq 1000$ Hz,
- PWM inverter harmonics situated around the switching frequency (4500 – 5500 Hz).

All these components should generate electromagnetic vibrations because of the quadratic transfer function described in section I. Therefore, radial vibrations, which contains electromagnetic vibrations, should contain common spectral components

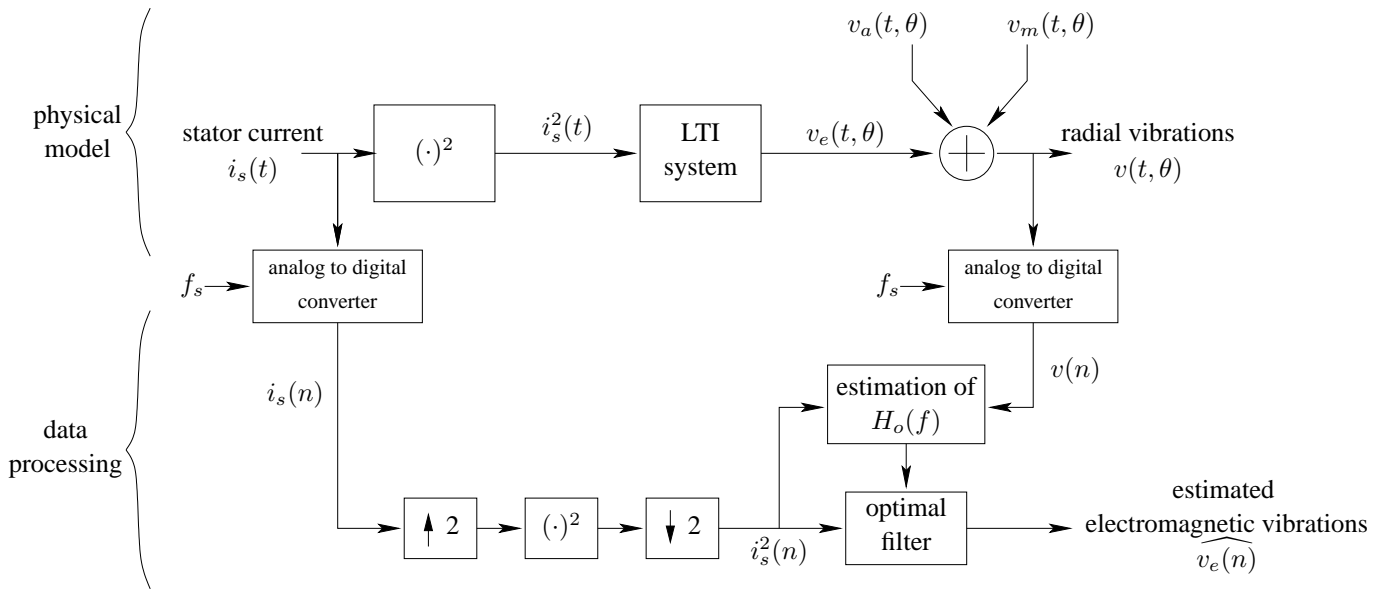


Fig. 2. Schematic representation of the complete algorithm

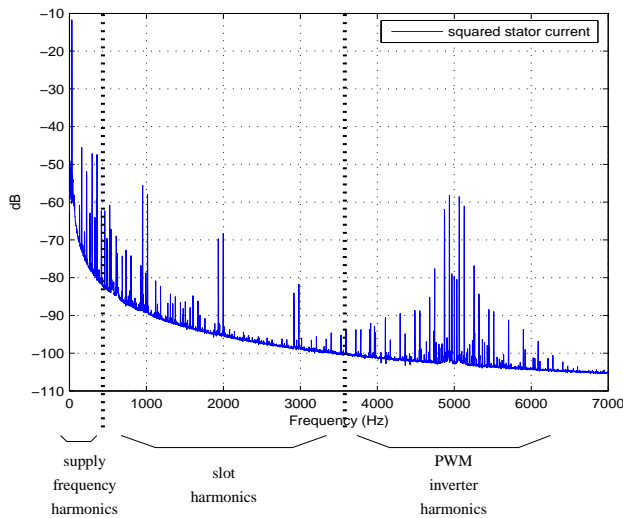


Fig. 4. PSD of one stator current

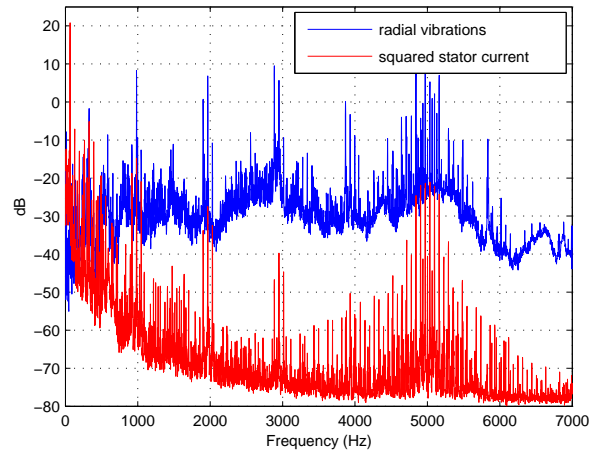


Fig. 5. PSD of one squared stator current and radial vibrations

with squared stator currents. The PSD of these two signals are compared in Fig 5, where strong common components appear, particularly for slot and PWM harmonics.

These common components, contained in measured radial vibrations, should be identified by the algorithm presented in section II as electromagnetic vibrations. The obtained results are presented in Fig. 6, where the PSD of measured radial vibrations $v(n)$ (blue curve) is compared with the PSD of estimated electromagnetic vibrations $\widehat{v_e(n)}$ (red curve) in the upper figure, and with the PSD of estimated non-electromagnetic vibrations $\widehat{v_a(n) + v_m(n)}$ (red curve) in the lower figure. The upper figure shows that the proposed algorithm correctly estimates PWM components and slot harmonics as electromagnetic vibrations which is a quite good result. In the lower figure, it can be seen that all the previous components, induced by stator currents, have been canceled from estimated non-electromagnetic vibra-

tions $\widehat{v_a(n) + v_m(n)}$. This last signal is now mainly constituted by a wide band component due to aerodynamic phenomena and some spectral lines due to mechanical phenomena [1], [2].

In order to study these results more precisely, the previous spectral quantities are analysed for three different narrow frequency bands in the following figures.

First, the previous PSD are analyzed around the supply frequency in Fig. 7, *i.e.* in the low frequency band (0 – 300 Hz). The PSD of radial vibrations (blue curves) is composed of several harmonics added with wide band components. These different components has the following physical origins [1], [2]:

- one mechanical harmonic with frequency $f_r = 13.7$ Hz, due to the natural mechanical excentricity of the machine,
- one electromagnetic harmonic with frequency $2 \times f_s = 64$ Hz due to the squared stator current fundamental component,
- some wide band components due to aerodynamic phenom-

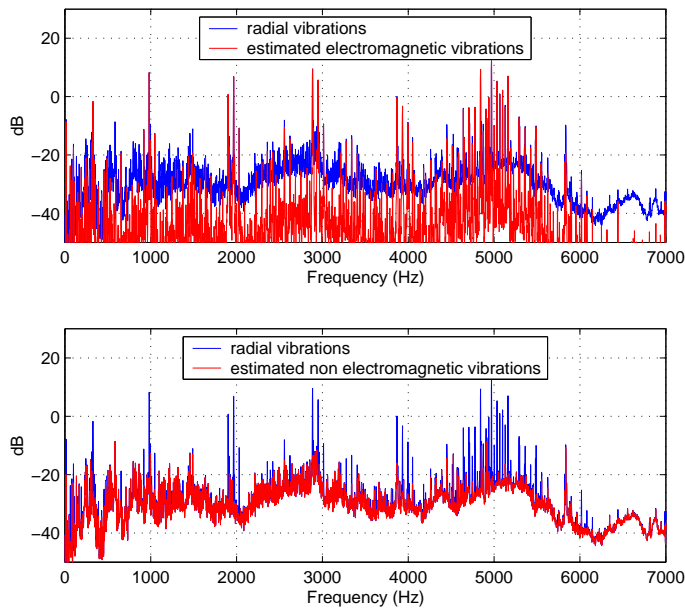


Fig. 6. PSD of real vibration signals: wide band results

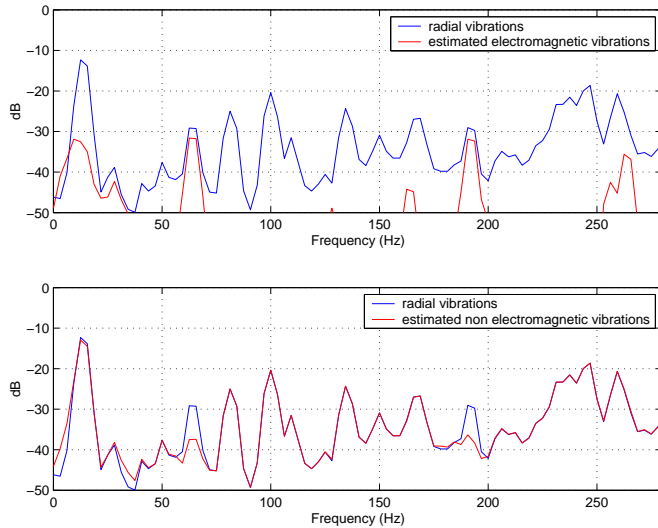


Fig. 7. PSD of real vibration signals: low frequency band

ena,

- other small harmonics.

After processing, the first harmonic (13.7 Hz) is well identified as a mechanical component since it has been removed from the PSD of estimated electromagnetic vibrations (upper figure, red curve), and is present in the PSD of estimated non-electromagnetic vibrations (lower figure, red curve). On the contrary, Fig. 7 shows that the proposed algorithm well identifies the second harmonic as an electromagnetic component. It can be noted that a similar result is obtained for another small harmonic component with frequency $6 \times f_s = 192$ Hz. This last result comes from the fact that the transfer function between stator currents and electromagnetic vibrations is quadratically nonlinear, and induces cross products between different stator currents components. Indeed, this particular term is created by the cross product between the stator currents funda-

mental harmonic (frequency f_s) and its 5th and 7th harmonics ($5f_s + f_s = 7f_s - f_s = 6f_s = 192$ Hz). Finally, aerodynamic wide band components (for example around 250 Hz) are correctly identified as non-electromagnetic vibrations.

The second analyzed frequency band is between 1800 Hz and 2300 Hz (middle frequency band), and the corresponding PSD are shown in Fig. 8. They contain three main spectral lines lo-

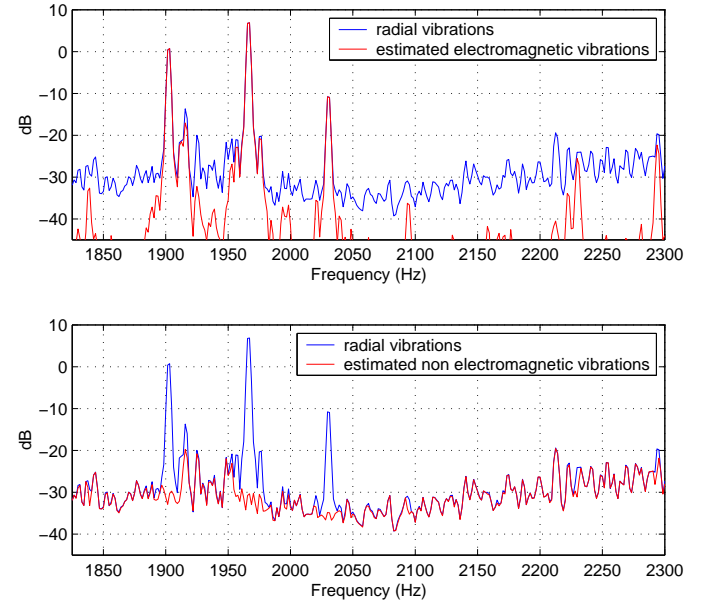


Fig. 8. PSD of real vibration signals: middle frequency band

cated at frequencies 1910 Hz, 1970 Hz and 2035 Hz, which can be identified as slot harmonics. Indeed, for this induction machine, these harmonics are located at $k \times 24f_r + n \times 2f_1$ Hz (k integer, $n = 0, \pm 1$) [1], [2], which corresponds to the previous frequencies with $k = 6$. These components, clearly visible in the DSP of the measured radial vibrations $v(n)$, have an electromagnetic origin since they are generated by currents slot harmonics. They are correctly estimated as electromagnetic components by the proposed algorithm, and completely removed from the DSP of estimated non-electromagnetic vibrations $\widehat{v_a(n)} + \widehat{v_m(n)}$. On the contrary, wide band component, mainly due to aerodynamic vibrations, is correctly identified as non-electromagnetic vibrations.

Third, Fig. 9 shows the results obtained around $f_{PWM} = 5$ kHz, the switching frequency of the PWM inverter (high frequency band). It is well known that such an inverter generates an important number of harmonics around its switching frequency. This figure shows that the proposed algorithm identifies these harmonics as electromagnetic vibrations components, and completely remove them from the estimated non-electromagnetic vibrations PSD.

For the sake of clarity the previous results are presented in the frequency domain. However, the proposed algorithm is able to estimate electromagnetic and non-electromagnetic vibrations signals in the time domain. Their time representations, given in Fig. 10, show that measured radial vibrations $v(n)$ are mostly composed of electromagnetic vibrations $v_e(n)$ at this location on the stator frame. Indeed, the power of $v_e(n)$ can now be

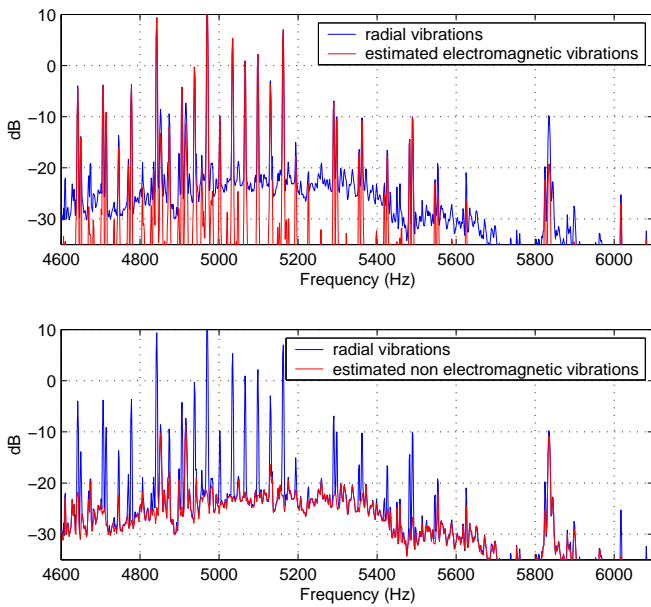


Fig. 9. PSD of real vibration signals: high frequency band

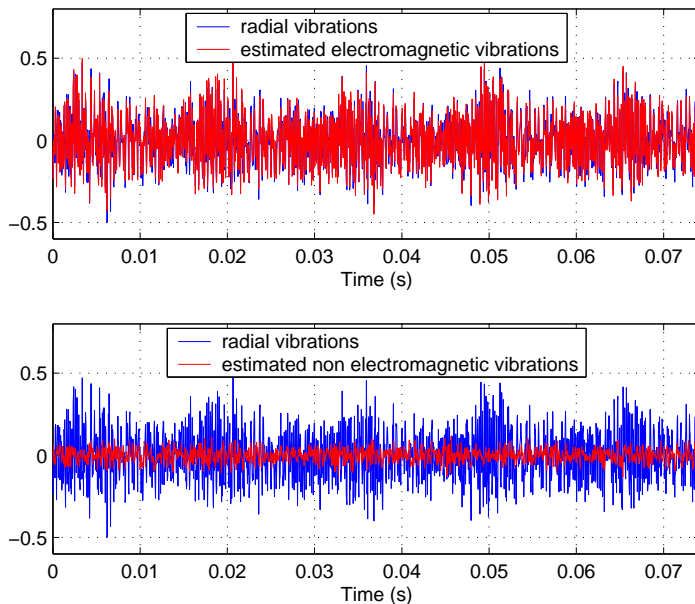


Fig. 10. Time domain results

correctly estimated, and represents 93% of the power of $v(n)$ at this location. This is not surprising since the chosen location is the middle of the stator frame, where electromagnetic effects are predominant with respect to mechanical effects.

IV. CONCLUSION

The aim of this work was to develop an algorithm able to extract electromagnetic vibrations from radial vibrations and stator currents of an induction machine. This was done thanks to the physical nonlinear model existing between these quantities. The proposed algorithm estimates an optimal nonlinear filter thanks to classical spectral quantities (cross and auto spectra), in order to modelize the previous nonlinear system. This algorithm, able to estimate electromagnetic and non-

electromagnetic vibrations in the time domain, has been applied to real signals, and the obtained results are very satisfactory. It can be noted that this algorithm was developed for steady state operating conditions, but can be easily extended to a nonstationary context thanks to adaptive filtering techniques.

The obtained results are particularly interesting in order to understand and analyze the vibratory influence of the inverter PWM strategy used to control the machine. This algorithm can also be viewed as a denoising operation applied to radial vibrations in order to remove all electromagnetic vibrations. Indeed, the denoised signal, constituted by estimated aerodynamic and mechanical vibrations $\widehat{v_a(n)} + \widehat{v_m(n)}$ can be further processed in order to detect more easily mechanical or aerodynamic defects such as bearing faults, rotor unbalanced, fan faults, etc.

REFERENCES

- [1] P.L. Timar, *Noise and vibration of electrical machines*, Elsevier Science Pub. Co., 1989.
- [2] S.J. Yang, *Low-noise electrical motors (monographs in electrical and electronic engineering)*, Clarendon Press, 1981.
- [3] G. Henneberger et al., "Procedure for numerical computations of mechanical vibrations in electrical machines," *IEEE Trans. on Magnetics*, 1992.
- [4] D.H. Im et al., "Analysis of radial force as a source of vibration in an induction motor with skewed slots," *IEEE Trans. on Magnetics*, 1997.
- [5] R. E. Crochiere and L. R. Rabiner, "Interpolation and decimation of digital signals - a tutorial review," *Proceedings of the IEEE*, vol. 69, no. 3, pp. 300-331, March 1981.
- [6] B. Widrow et al., "Adaptive noise cancelling: principles and applications," *Proceedings of the IEEE*, 1975.
- [7] B. Widrow and S. D. Stearns, *Adaptive signal processing*, Prentice Hall, 1985.
- [8] J. L. Lacoume and J. Max, *Méthodes et techniques de traitement du signal et applications aux mesures physiques*, Masson, 1996.
- [9] P. J. Brockwell and R. A. Davis, *Time series: theory and methods*, Springer series in statistics, 1991.